Title
VIBRATIONS, SPBCTROSCOPY OF HYDROGEN ADSORBED ON METAL SURFACES

Authors
Mate, CM.
Bent, B.E.
Somorjai, G.A.

Publication Date
1985-10-01

Lawrence Berkeley Laboratory
UNIVERSITY OF CALIFORNIA

Materials & Molecular Research Division

To be published as a chapter in Hydrogen in Catalysis - Theoretical and Practical Aspects, Z. Paal, Ed., Marcell Dekker, Inc., New York, New York, 1986

VIBRATIONAL SPECTROSCOPY OF HYDROGEN ADSORBED ON METAL SURFACES

C.M. Mate, B.E. Bent, and G.A. Somorjai

October 1985

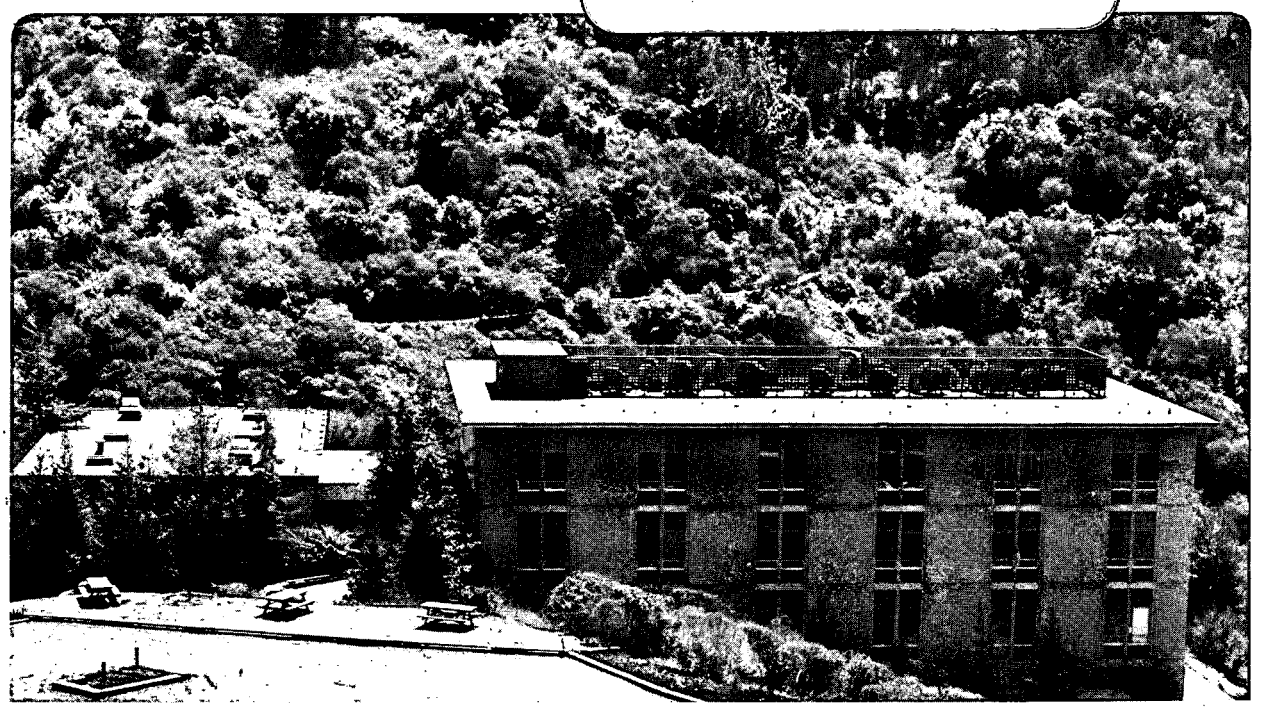

Prepared for the U.S. Department of Energy under Contract DE-AC03-76SF00098

DISCLAIMER

LBL-20361

VIBRATIONAL SPECTROSCOPY OF HYDROGEN ADSORBED ON METAL SURFACES

C.M. Mate, B.E. Bent, and G.A. Somorjai

Materials and Molecular Research Division
Lawrence Berkeley Laboratory
and
Department of Chemistry
University of California
Berkeley, California 94720

October 1985

VIBRATIONAL SPECTROSCOPY OF HYDROGEN ADSORBED ON METAL SURFACES*

C.M. Mate, B.E. Bent, and G.A. Somorjai

Materials and Molecular Research Division and Department of Chemistry
University of California
Berkeley, California 94720

OUTLINE

I. Introduction.....2

II. High-Resolution Electron Energy Loss Spectroscopy of Hydrogen Adsorbed on Metal Single Crystal Surfaces in Ultra-high Vacuum.....3

a. Dipole Scattering.....5

b. Impact Scattering.....6

c. Site Determination by HREELS.....8

d. Delocalized Hydrogen.....10

e. Trends in the HREEL spectra.....15

III. Vibrational Spectroscopy of Hydrogen Adsorbed on High Surface Area Metals at Atmospheric Pressures.....18

a. Incoherent Inelastic Neutron Scattering.....18

b. Infrared and Raman Spectroscopy.....20

IV. Conclusions.....22

* To be published in Hydrogen in Catalysis - Theoretical and Practical Aspects, Z. Paal, ed., as a book chapter.

I. Introduction

Vibrational spectroscopy is essentially the study of atomic motion. A bound atom, either in a molecule or to a surface, undergoes quantized vibrational motion, and the vibrational frequencies are measurable by vibrational spectroscopy.

In surface reactions, atoms have to move from site to site as well as break bonds and form new ones, so a knowledge of atomic motion is an important part of any atomic scale understanding of the chemical processes. Further, since the vibrational frequencies reflect the symmetry of atomic motion and the nature of interatomic potentials, vibrational spectroscopy provides an excellent insight into the bonding environment of atoms and molecules.

Over the last 25 years, a number of vibrational spectroscopies have achieved sufficient sensitivity to measure vibrations of adsorbates on surfaces(1-13); these techniques are listed and described in Table 1. In this review, we examine the vibrational spectroscopies used to study hydrogen adsorption on metal surfaces, which are the first five spectroscopies listed in Table 1 - HREELS, IINS, RAIRS, TAIRS, and Raman spectroscopy.

First, we review what is presently known from vibrational spectroscopy about adsorption of hydrogen in ultra-high vacuum (UHV) on well-defined single crystal surfaces. Here, the preferred technique of investigation is high-resolution electron energy loss spectroscopy (HREELS). Next, we review the adsorption of hydrogen at atmospheric pressure on samples that have a high surface to volume ratio and that are similar to the metal surfaces of heterogeneous catalysts used in industry. Here, the results are primarily from incoherent inelastic neutron scattering, infrared spectroscopy, and Raman spectroscopy.

II. High-Resolution Electron Energy Loss Spectroscopy of Hydrogen Adsorbed on Metal Single Crystal Surfaces in UHV

Much of our atomic scale understanding of how hydrogen interacts with metal surfaces has come from experiments studying hydrogen chemisorption on single crystal surfaces under ultra-high vacuum conditions. Ultra-high vacuum (i.e. gas pressures less than 10^{-8} torr) is necessary to ensure that a substantial quantity of gases other than hydrogen do not adsorb on the metal surface during the course of an experiment. By studying hydrogen on atomically clean single crystal surfaces, one can learn how hydrogen interacts with well-characterized metal surfaces, an important starting point to an eventual understanding of how hydrogen behaves on the less well-defined surfaces present on high-surface-area catalysts.

Single crystal surfaces make it possible to study the bonding of hydrogen on surfaces with different types of adsorption sites. Figure 1 shows some of the low-Miller-index crystal surfaces of face-centered cubic (fcc), body-centered cubic (bcc), and hexagonal close-packed (hcp) metals; top sites, bridge sites, 3-fold and 4-fold hollow sites are indicated.

The most important vibrational spectroscopy currently used to study hydrogen adsorbed on single crystal surfaces is high-resolution electron energy loss spectroscopy (HREELS). Most HREEL spectrometers have a high sensitivity to adsorbates and obtain spectra over the entire vibrational frequency range (100-5000 cm^{-1}) in less than 20 minutes, which accounts for the widespread use of HREELS to study all types of adsorbates on single crystal surfaces. These attributes are particularly important for studying adsorbed hydrogen, since hydrogen is difficult to detect with many experimental probes. HREELS is able to detect a few percent of a monolayer of hydrogen adsorbed on a single crystal surface. Also, for adsorbed hydrogen, a large frequency

range is necessary, since the vibrational frequencies observed can range from 400 cm^{-1} for atomic deuterium chemisorbed on hexagonally close-packed metal surfaces [14] to 4159 cm^{-1} for the H-H stretching mode of molecularly adsorbed hydrogen [15].

Figure 2 shows a HREEL spectrometer used by the authors which is also typical of spectrometers in current use. The monochromator produces a beam of low-energy electrons (1-10 eV) which is focussed on the sample. The energy and angle of the scattered electrons are then determined by the analyzer. Most (99.9%) of the electrons incident on a metal single crystal surface are reflected elastically without any change in energy, but a fraction of the electrons scatter inelastically; that is they lose energy by exciting a vibrational mode of an adsorbate or of some other surface excitation. For vibrational excitations, the energy lost by the exciting electron is relatively small in comparison to the energy of the incident electron beam, so the spectrometer must be able to operate at fairly high resolution, typically less than 10 meV or 80 cm^{-1} (1 meV = 8.0655 cm^{-1}), in order to distinguish the weak loss peaks from the intense peak of elastically scattered electrons; hence the name of the technique -- High-Resolution Electron Energy Loss Spectroscopy. A large number of reviews [16] and several excellent books [5] have been written on the design of HREEL spectrometers and their application to the study of atoms and molecules adsorbed on surfaces.

In 1967, Propst and Piper reported the first vibrational spectra, obtained by HREELS, of adsorbates on a metal surface, W(100) [17]. Among the gases adsorbed in this experiment on the W(100) surface was hydrogen. Since then the study of hydrogen adsorbed on W(100) by HREELS has played a central role both in the development of HREELS and in studies of adsorbed hydrogen. We use this system to illustrate how vibrational fre-

quencies measured by HREELS are used to determine adsorption sites on a well-defined metal surface. Making this assignment requires first an understanding of the mechanisms of vibrational excitation by electron scattering from adsorbate-covered surfaces [18-29]. According to our present views, these mechanisms can be conveniently divided into two categories: a long-range scattering process called dipole scattering and a short-range scattering process called impact scattering.

II.a. Dipole Scattering

Dipole scattering is similar in nature to the vibrational excitation mechanism in infrared (IR) vibrational spectroscopy. The long-range Coulomb field of the incident electrons interacts with the "dynamic dipole" of a vibrating adsorbate just as the electric field of the incident photons in IR spectroscopy interacts with the dynamic dipole of a molecule. This coupling between the electron and the dynamic dipole moment of the adsorbate enables the electron to lose a quantum of energy by exciting an adsorbate vibrational mode.

An important characteristic of dipole scattering arises from the physical nature of the Coulomb field of the incident electron at the metal surface. Electric fields can only have a component perpendicular to a metal surface since parallel components are screened by the metal. Therefore, only the component of the dynamic dipole moment perpendicular to the surface can couple with incoming electrons. This results in what is usually called the "surface dipole selection rule" which states that only vibrations which have a net dynamical dipole moment perpendicular to the surface can scatter electrons via the dipole scattering process.

Another charateristic of dipole scattering, which enables one to distinguish between dipole and impact scattering processes, is the angular dependence of the scattering intensity; the dipole scattering intensity

falls off rapidly for scattering angles away from the specularly reflected electron beam. The angular halfwidth of the dipole scattering intensity is on the order of $\hbar\omega_o/2E_I$, where ω_o is the frequency of the vibration and E_I is the incident electron energy. In typical HREELS experiments, the dipole scattered electrons are concentrated within a couple degrees of the specular beam.

A good example of dipole scattering is the 130 meV (1050 cm^{-1}) loss that appears in the HREEL spectra for a saturation coverage of hydrogen atoms on the unreconstructed surface of W(100). As shown in Figure 3, there is an intense loss at 130 meV for spectra obtained in the specular direction. Figure 4 shows that the intensity of this loss decreases with sample rotation as the analyser collects electrons scattered at angles away from specular direction. This angular dependence of the scattered intensity allows us to identify the 130 meV loss with a dipole active vibrational mode; then, using the surface dipole selection rule, we can conclude that the 130 meV loss corresponds to the vibration of hydrogen perpendicular to the surface.

II.b. Impact Scattering

Figure 3 also shows that, at off-specular collection angles, several other weak losses are visible in the HREEL spectrum. These losses are the result of vibrational modes parallel to the surface being excited by impact scattering. During the impact scattering process, the incident electrons lose energy by interacting directly with the atomic potentials while the electrons are within a few Ångstroms of the surface. During this very short-range interaction, the electrons essentially become "impacted" in the surface atoms for a short period of time, allowing vibrational modes oriented parallel to the surface, as well as those oriented perpendicular, to be excited by the electrons. Figure 4 shows that the losses from the parallel vibrational

modes of hydrogen atoms on the W(100) surface have a broad angular distribution, characteristic of impact scattering and unlike the narrow angular distribution of dipole scattering.

This short-range, impact scattering is physically a much more complicated process than the long-range dipole scattering process. The complicated nature of impact scattering is well-illustrated by the HREEL spectra for hydrogen adsorbed on Rh(111) [30]. For this system the loss peaks in the vibrational spectra show interesting intensity variations with changes in the incident electron beam energy. Figure 5 shows the HREEL spectra for a saturation coverage of hydrogen on Rh(111) taken at several different incident electron energies, while Figure 6 shows how the intensities of the elastic peak and of the three main losses in the specta vary as a function of incident electron energy. All three loss peaks have maximum intensity at ~4.7 eV while the elastic peak shows maximum intensity at ~2 eV. Further, this maximum intensity at 4.7 eV is due to impact scattering as determined by measuring the angular distribution of these peak intensities at different incident beam energies. For incident energies less than about 3 eV, the loss intinsities fall off dramatically at angles away from the specular direction indicating dipole scattering as the main scattering mechanism in this energy range. Above 3 eV, however, the angular distribution of the loss intensities is fairly broad implicating impact scattering as the main scattering mechanism at these energies. The loss intensity maxima at ~4.7 eV are attributed to a "resonant" impact scattering off the atomic potentials. While resonant impact scattering is poorly understood at present, resonant electron scattering from gas phase atoms and molecules has been studied extensively where it is thought to involve the temporary capture of the incident electron to form a short-lived negative ion [31].

Even though the mechanism of impact scattering is not as well understood as that for dipole scattering, a detailed knowledge is fortunately usually not required in order to interpret HREEL spectra; in most cases, it suffices to know only whether a particular mode has some dipole scattering contribution and, consequently, a net dynamic dipole perpendicular to the surface. Impact scattering does have, however, some useful selection rules which apply in certain cases [32]:

1) The inelastic scattering intensity vanishes for a vibration that is odd with respect to a mirror plane symmetry if trajectories of both the incident and scattered electrons lie in this symmetry plane.

2) The inelastic scattering intensity vanishes in the specular direction for a vibration that is odd with respect to a mirror plane symmetry if the plane containing the trajectories of the incident and scattered electrons is perpendicular to the mirror plane and the surface.

3) The inelastic scattering intensity vanishes in the specular direction for a vibration that is odd with respect to a two-fold rotation symmetry.

II.c. Site Determination by HREELS

These selection rules for impact scattering, along with the surface dipole selection rule, help determine the symmetry of the hydrogen adsorption site [21,23,24,26,29]. To illustrate this point, we again use the case of hydrogen adsorbed on the W(100) crystal surface. As shown in Fig. 2, a total of four losses are observed, with energies of 80, 130, 160, and 260 meV, resulting from dissociatively adsorbed hydrogen. Since the 260 meV loss has twice the energy of the 130 meV loss, it is probably an overtone or multiple loss of the 130 meV loss. The remaining three losses (80, 130, and 160 meV) come from the motion of hydrogen atoms on the surface.

If we assume that the hydrogen atoms are well-localized on the surface, then these three losses correspond to the three vibrational modes of hydrogen atoms bound at a particular type of site or sites. An atom bound to a surface has three "normal modes" of vibration, since a free atom has three degrees of freedom. At least one of these vibrational modes must involve motion of the atom perpendicular to the surface. Since only the 130 meV mode is dipole active, one can conclude that there is only one type of adsorption site. The 80 meV and 160 meV modes are not dipole active, so they correspond to vibrations parallel to the surface, and since the 80 and 160 meV losses are not seen in the specular direction (Figure 3A), they must satisfy one of the selection rules of impact scattering. Of the possible point groups for a hydrogen atom on W(100) - C_{4v}, C_{2v}, C_s, and C_1- only for C_{2v} can adsorbed hydrogen have two non-degenerate, non-dipole active vibration modes of the correct symmetry to satisfy the impact scattering selection rule. In this case, once we know the symmetry of the adsorption site, we also know the adsorption site, since a bridge site (as shown in Figure 1) is the only site on the W(100) surface with C_{2v} symmetry.

For H adsorbed on the W(100) surface, one can also determine bond lengths and bond angles from the vibrational frequencies by making the following assumptions: 1) The mass of the metal atoms is infinite, 2) The bonds between the hydrogen and the metal atoms can be approximated by springs, and 3) the angle-bending force constant is much smaller than the bond-stretching constant. If ν_{sym} is the vibrational frequency perpendicular to the surface and ν_{as} is the vibrational frequency parallel to the surface along the M-H-M bond for hydrogen bound at a bridge site, then the M-H-M interbond angle, α, is related to the vibrational frequencies by $\nu_{as}/\nu_{sym} = \tan(\alpha/2)$. This theoretical relationship between

frequencies and bond angles has been applied to bridge bonded hydrogen atoms in metal hydrides [33] as shown in Figure 7 which plots the ν_{as}/ν_s ratio measured by IR spectroscopy versus the $\tan(\alpha/2)$ determined by x-ray or neutron diffraction. The correlation between the theoretical and experimental angles is quite good. Furthermore, for cluster hydrides, once the M-H-M bond angle is determined from the ν_{as}/ν_s ratio, one can determine the metal-hydrogen bond distance if the metal-metal separation is known.

Willis has applied this correlation for metal cluster hydrides to surfaces to determine bond angles and bond lengths for hydrogen on W(100) [23]. The ν_{as}/ν_s ratios for hydrogen on unreconstructed p(1x1) W(100) and on reconstructed c(2x2) W(100) are also plotted in Figure 7. Figures 8A and 8B show the bonding geometries determined from Figure 7 for hydrogen atoms on W(100). It is noteworthy that a specific surface site (bridge site, for example) does not have "characteristic" vibrational frequencies. Within a given adsorption site, small changes in bond lengths and bond angles have a large effect on the measured vibrational frequencies as demonstrated in Figure 7 by the variation from one to two in the ν_{as}/ν_s ratio for bridge-bonded hydrides.

II.d. Delocalized Hydrogen

For hydrogen adsorbed on W(100), it is fairly straightforward to determine the bonding geometry using HREELS.* For hydrogen adsorbed on other metal surfaces this is not always possible for several reasons. 1) The selection rules for impact scattering do not apply in every experimental situation. 2) Hydrogen is a weak scatterer of electrons so often a vibrational mode is too low in intensity to be detectable. 3) The hydrogen atoms may not be well-localized at an adsorption site in which case the atomic motion no

*However, a recent publication [34] indicates that a new assignment of the the HREEL spectrum for H on W(100) will be proposed in a future publication.

longer approximates that of a simple harmonic oscillator.

The last effect is somewhat unexpected and has only recently been discussed in the literature [30,35,36,37]. This effect arises because vibrating hydrogen has a large displacement amplitude, and because the potential energy of hydrogen on a surface does not go to infinity parallel to the surface as it does, to a good approximation, perpendicular to the surface. Instead, a finite potential barrier exists between the energetically favorable adsorption sites. If the ground state vibrational energy is on the same order as the barrier height, then it is possible for hydrogen to tunnel from one site to another. Also, the energy of the excited vibrational states can be larger than the height of the barrier potential in which case it is no longer valid to think of small vibrations about an equilbrium position; instead, one should think of the atom moving across the surface with a certain momentum and with its motion perturbed by the periodic potential of the surface. The phenomena is analogous to electrons in solids where their motion is described by energy bands.

For electrons in solids, there are two physical models which are commonly used to explain the formation of energy bands and band gaps. One model, called the free-electron model, treats the electrons in the solid as a free-electron gas and the periodic potential of the lattice as a perturbation on the free electron energies. The second model, called the tight binding method, approximates the electron states as the atomic orbitals of the free atoms. In this second model, the bands occur from the overlap of orbitals of neighboring atoms. While one can show that the two models are equivalent ways of looking at the same physical problem, one usually obtains a better intuitive understanding of how electrons behave in a solid by using the free-electron model when the periodic

potential seen by the electrons is small compared to their energy and by using the tight binding method when the electron energies are smaller than the maximum potential energy between atoms.

Therefore, for the lowest energy bands of hydrogen adsorbed on metal surfaces, the tight binding method would provide the best understanding of the nature of these bands. In this method one first determines the wavefunctions that are solutions of the Schroedinger equation for a potential well centered over a particular site. Since the wavefunctions still have a finite value at distances away from the center of the site, a fraction of each wavefunction will overlap to a certain extent with the wavefunctions of neighboring sites. The wavefunctions of neighboring sites are degenerate in energy with those of the original sites before the overlap is taken into account since the potential wells of the neighboring sites are the same as the original site; however, the overlap of wavefunctions lifts the degeneracies, resulting in the formation of energy bands.

For hydrogen adsorbed on W(100), the separation distance between neighboring bridge sites is fairly large (3.16 Å), so the overlap of wavefunctions is probably small. Therefore, the low energy bands of hydrogen on W(100) should be fairly narrow, and the wavefuntions well-localized at bridge sites. Consequently, even for such "localized" hydrogen atoms, the previous analysis would be valid.

However, other types of crystal faces can have adsorption sites with substantially smaller separation distances. Consequently, the overlap of even the ground state wavefunctions on these surfaces can be significant, leading to broad energy bands. In this case, the hydrogen atoms are not well-localized at adsorption sites but instead can tunnel from site to site.

Recently, Puska et al [36,37] have calculated the low-energy position wavefunctions for hydrogen adsorbed on the Ni(100), Ni(111) and Ni(110) surfaces where the distance between hollow sites is, respectively, 2.49 Å , 1.44 Å ,and 1.44 Å. These calculations use the effective-medium approximation of density functional theory to calculate the potential energy of hydrogen on the these surface. The Schroedinger equation is then solved numerically to determine the wavefunctions. Figure 9A shows the potential energy and the A_1 wavefunctions, and densities for hydrogen chemisorbed on the Ni(100) surface; Figure 10 shows the corresponding band structure for the A_1 wavefunctions of hydrogen chemisorbed on the Ni(100) surface. The lowest energy wavefunction (Fig. 9C) is fairly well-localized at the hollow sites but the wavefunctions of the first two excited bands (Figs. 9E, 9G) are substantially less localized. The wavefunctions of the excited bands correspond to motion both perpendicular and parallel to the surface. The coupling between the perpendicular and parallel motion results from the anharmonicity of the potential well, as shown in Figure 9B, over the distance of the zero point motion of the hydrogen atom.

Table 2 lists the calculated band centers and bandwidths for hydrogen on Ni(111). The bandwidths are larger than those calculated for Ni(100) because the smaller separation distances between hollow sites on this surface results in more overlap of neighboring wavefunctions. Since the lowest energy band is fairly narrow (~4 meV), this band will be fully occupied, even at liquid nitrogen temperatures, but the higher energy band will only be sparsely occupied at this temperature. Consequently, the losses observed in HREELS for hydrogen adsorbed on this surface would correspond to transitions from all parts of the Brillouin zone of the first band to higher energy bands; the transitions are "vertical",

since, for HREEL spectra obtained in the specular direction, $\Delta k_{\parallel} = 0$.

Table 2 also lists the experimentally observed values for transitions between bands for hydrogen adsorbed on several hexagonally close-packed surfaces. Off specular measurements indicate that the 820 and 1140 cm^{-1} transitions of hydrogen on Ru(001), the 750, 1100, and 1430 cm^{-1} transitions of hydrogen on Rh(111) and the 550 cm^{-1} transition on Pt(111) are dipole active, so these excitations correspond to $A_1^{\circ} \rightarrow A_1^{n}$ transitions. The remaining observed excitations listed in Table 2 occur predominately by impact scattering. Since there could be a small dipole scattering contribution to these losses, it is not clear whether they should be assigned to $A_1^{\circ} \rightarrow E^{n}$ transitions which are not dipole active or to dipole active $A_1^{\circ} \rightarrow A_1^{n}$ transitions. These frequencies have been assigned by us, somewhat arbitrarily, to transitions that are closest to those predicted theoretically for hydrogen on Ni(111). Many of the transitions that are predicted to occur have not been observed, most likely due to very low excitation probabilities For hydrogen adsorbed on Rh(111), all the low-energy transitions have been observed by choosing incident beam energies that enchance the various excitation probabilities.

The observation of all the low-energy transitions for the motion of hydrogen on the Rh(111) surface is strong experimental evidence that the hydrogen atoms are fairly delocalized on this surface. Further, when deuterium is adsorbed instead of hydrogen on Rh(111), the band positions and bandwidths undergo isotopic shifts that do not correspond to those predicted by a simple harmonic oscillator model; however, the shifts do fit a model where the motion parallel to the surface is that of a free atom perturbed by a periodic potential [30].

IIe. Trends in the HREEL spectra

Except for HREEL spectra of H_2 physisorbed on Cu and Ag at 10 K [15], HREEL spectra of H_2 adsorbed on transition metal surfaces from 70-300 K show dissociative adsorption of H_2. Tables 2 and 3 summarize the vibrational frequencies observed for hydrogen chemisorbed on metal single crystal surfaces. No vibrational frequencies for hydrogen bonding below the surface (for example between the first and second layers of metal atoms) have been reported. In most cases, the vibrational frequencies in Tables 2 and 3 are relatively insensitive to coverage, varying by at most 25 cm^{-1} as a result of lateral interactions [46a]. However on Ni(110), W(100), and Mo(100) the vibrational frequencies for adsorbed H change dramatically with coverage as a result of surface reconstructions. The metal atoms on these surfaces are induced by H adsorption at certain coverages to adopt new equilibium positions. This change in metal surface geometry, as we show below, greatly affects the H-atom bonding geometry and thus the vibrational frequencies.

Assigning the observed vibrational frequencies in Tables 2 and 3 and determining the adsorbed state of the hydrogen atoms is not straightforward. It appears that H atoms on the hexagonally close-packed surfaces tend to be delocalized parallel to the surface as supported by the assignments in Table I and their agreement with the calculations for Ni(111) [36,37]. Since this delocalization results from the overlap of the wavefunctions of H atoms in adjacent sites, surfaces with larger corrugation or with a greater distance between favored adsorption sites may bond H-atoms to a greater degree at localized sites. The bonding of H atoms in bridge sites on W(100) is a good example of this localized adsorption.

For hydrogen chemisorbed on other surfaces, the interpretation of the observed vibrational frequencies is less clear. The most common approach is to use a localized, valence-force field interpretation such as was used to

describe hydrogen on W(100). Table 3 includes proposed sites for H adsorption based on this assumption. It is not clear, however, whether the wavefunctions are localized enough on these surfaces for this approach to be valid. For example, on Ni(100) the only observed loss (at 74 meV, 595 cm^{-1}) was attributed by Andersson [43] to a vibration of the H atoms perpendicular to the surface in a four-fold hollow site. However, this frequency also agrees reasonably well with the calculated energy of transition between the A_1 and A_1 bands (62 meV) for delocalized hydrogen on Ni(100) [36,37]. Even though the calculations of Puska et al predict five transitions in the range of frequencies studied, the observation of only one loss for hydrogen on the Ni(100) surface may be due to low excitation probabilities for these other transitions.

It should be noted that even for "delocalized" H adsorption, certain surface sites will have a higher probability of occupation than others as shown in the right panel of Figure 9. For example, dynamical low-energy electron diffration (LEED) calculations have determined that H atoms bond in 3-fold hollow sites on Ni(111) [35]. The M-H bond length determined by LEED of 1.84 Å compares favorably with that of 2.05 Å for H on W(100) as determined by HREELS [23], since the covalent radius of W is .15 Å longer than that of Ni.

Despite the difficulties in interpreting the HREEL spectra of adsorbed H atoms, some general observations are possible. First, the vibration of a hydrogen atom perpendicular to the surface shifts to lower frequency with increased coordination to the metal [51]. Thus, $\omega_\perp$ for top site > bridge site > 3-fold hollow site > 4-fold hollow site. Secondly, the observed vibrational frequencies are highly sensitive to the local bonding geometry [51], as shown in Figure 7 for bridge-bonded H atoms in hydrides. Thirdly, the

local bonding geometry of hydrogen atoms and, thus, the observed vibrational frequencies are sensitive to the geometry of the metal. This can be seen by comparing the vibrational frequencies observed for H on the (111), (100), and (110) faces of Ni and W. For these two metals it appears that higher corrugation of the surface favors lower coordination of the H atom. For example, on the rough W(111) surface, H bonds to top sites versus bridge sites on the smoother W(100) and W(110) surfaces and, on the bumpy Ni(110) suface, H bonds to bridge sites versus 3- and 4-fold hollow sites on Ni(111) and Ni(100). Finally, metals towards the left of the transition metal series (W, Mo, Fe) seem to favor lower coordination of H atoms than those on the right (Pt, Pd, Ni).

It is interesting to try to correlate the vibrational frequencies to other physical parameters of adsorbed hydrogen. One parameter that has been measured for hydrogen adsorbed on many single crystal metal surfaces is the heat of adsorption. Tables 2 and 3 list the heats of adsorption of hydrogen on metal surfaces along with the observed vibrational frequencies. Only the heats of adsorption for low hydrogen coverages are listed since, at high coverages, lateral interactions become important and can complicate the interpretation of the data. For hexagonally close-packed surfaces, the heats of adsorption vary dramatically from 9.5 kcal/mole for hydrogen on Pt(111) to 29 kcal/mole for hydrogen on Ru(001), even though the vibrational frequencies of chemisorbed hydrogen are similar on these surfaces. This suggests that the vibrational modes are more sensitive to the structure of the crystal face than to the strength of the hydrogen-metal bond. Further evidence for this can be found by comparing different crystal faces of the same metal; the vibrational spectra are quite different for hydrogen adsorbed on the different crystal faces of nickel and tungsten, even though the

heats of adsorption do not change dramatically from one crystal face to another on these metals.

III. Vibrational Spectroscopy of Hydrogen Adsorbed on High Surface Area Metals at Atmospheric Pressure

While vacuum conditions are necessary for electron spectroscopies such as HREELS, several techniques - Incoherent Inelastic Neutron Scattering, Transmission-Adsorption Infrared Spectroscopy, Reflection-Adsorption Infrared Spectroscopy, and Raman Spectroscopy - are able to do vibrational spectroscopy of the metal/gas interface at high gas pressures. Since these probes interact only weakly with atoms and molecules, it is often necessary to use samples with a large surface to volume ratio in order to be sensitive to surface adsorbates. Using samples with a large surface to volume ratio is not necessarily a disadvantage since the same type of samples are used in heterogenous catalysis; so these techniques are able to study hydrogen under conditions similar to those present in catalysis.

In what follows, we briefly discribe these techniques and review the results obtained for hydrogen adsorbed on metal surfaces.

III.a. Incoherent Inelastic Neutron Scattering (IINS)

In a neutron scattering experiment, the neutrons scatter by interacting with the nuclei of the atoms in the sample. As was the case for electrons in HREELS, a fraction of the neutrons lose energy, when they scatter, by exciting vibrational modes of the sample. Unlike HREELS where the electrons do not penetrate significantly beyond the surface, neutrons can easily transverse a sample; so to be useful as a surface probe, the adsorbate must have a cross section which is substantially larger than that of the substrate. Fortunately, the incoherent inelastic cross section of hydrogen is at least twenty times greater than that of any other common element, so it

is possible to obtain reasonable scattered intensity from hydrogen-containing adsorbates. Several good reviews [6] have been written on neutron scattering as well as its application to the study of adsorbates.

To date, only a few types of metallic surfaces have been used in neutron scattering experiments due to the difficulties in obtaining samples with both a clean and high-area surface. So far the adsorption of hydrogen has been studied by IINS on Raney nickel [52] and on platinum [53] and palladium blacks [54]. Table 4 gives a summary of the inelastic neutron scattering results obtained for hydrogen on these surfaces. A comparison of the frequencies observed for hydrogen adsorption on Raney nickel and platinum black with those obtained by HREELS for hydrogen on Ni(100), Ni(111), Ni(110), Pd(100), and Pt(111) shows that most of the HREELS frequencies are also observed in the neutron scattering experiments. This is probably due to hydrogen adsorption on the the same type of crystal faces in the high surface area samples. However, more modes are observed by IINS than by HREELS; these could be due to adsorption on different crystal surfaces and on imperfections such as steps or kinks or could be due to modes that are weak scatterers by HREELS (i.e. modes parallel to the surface) but that are relatively intense by IINS.

Since the surfaces used in IINS are less well defined than the single crystal surfaces used in HREELS, it is difficult to make a definite assignment of the observed frequencies. Most researchers have interpreted the IINS data for hydrogen adsorption in terms of localized harmonic oscillators at multi-coordinated sites. As was the case in interpreting HREEL spectra, however, hydrogen may not always be well approximated by a localised harmonic oscillator, but such an approximation is probably more valid for high surface area metals which have more defects and a larger surface corrugation than "smooth" single crystal surfaces. Further, most of the values for the transition energies

calculated by Puska et al [36,37] for delocalized hydrogen on Ni(100) and Ni(111) are in poor agreement with those observed in the neutron scattering experiments, implicating a more localized adsorption on these high-surface-area metals.

III.b. Infrared and Raman Spectroscopy

These spectroscopies, like IINS, offer both better spectral resolution than HREELS and the ability to study gas adsorption at atmospheric pressures on high surface area catalysts. IR and Raman spectroscopies are also less costly and more readily available than thermal neutron sources. However, because of the small dynamic dipole moment and small polarizability of metal-hydrogen bonds, measurement of the vibrational spectrum for chemisorbed hydrogen by IR or by Raman spectroscopy is difficult. Only a few metal/hydrogen systems have been studied, to date, and transmission absorption infrared spectroscopy (TAIRS) has been used in all but a few of these studies.

In TAIRS, an infrared beam is transmitted through the sample and its adsorption as a function of frequency is measured before and after the introduction of gas into the sample cell. The differences in the adsorption spectra gives the vibrational frequencies of the adsorbed species. In order to use this spectroscopy, it is important to have high surface area samples so that the spectra have a significant contribution from the surface. Also, it is important to have samples which have good transmission in the frequency range of interest. However, even with the most infrared transparent samples, the spectral range is limited to 1000-5000 cm^{-1}. For these reasons, TAIRS studies of adsorbed hydrogen have been limited to metal powders or metals dispersed on oxide supports that give high IR transmission and that have a high surface area.

Reflection absorption infrared spectroscopy (RAIRS) is similar to TAIRS except that the absorption of infrared radiation is detected by the change in

intensity of a reflected IR beam when an adsorbate is present on the reflecting surface. Samples must therefore be reflective and are generally polycrystalline foils or single crystals. The spectral range is limited by the transmission of the infrared windows to frequencies above 400 cm^{-1}. Recently, vibrational spectra of hydrogen adsorbed on a single crystal surface (W(100)) in ultra-high vacuum have been obtained using RAIS [34]; in the future, this technique promises to be an important competitor to HREELS for obtaining vibrational spectra of hydrogen adsorbed on single crystal surfaces. An excellent review of this spectroscopy has been written by Hoffmann [9].

The vibrational spectrum in Raman spectroscopy (reviewed [7,8]) is recorded by measuring the inelastic scattering of visible light. Raman spectroscopy has an even lower cross section for vibrational excitation of adsorbed hydrogen than IR spectroscopy, so high surface area samples like those for TAIRS are generally used. However, because visible, rather than infrared, light is used, supports are transparent to lower frequencies, and spectra down to 200 cm^{-1} can be obtained.

Table 5 gives a summary of the TAIRS, RAIRS, and Raman spectroscopy data for hydrogen adsorbed on high surface area metals and metals dispersed on oxide supports. All the frequencies observed are fairly high (>1800 cm^{-1}) in contrast to the lower values observed for hydrogen adsorption on unsupported metals. However, the lower frequency modes (<1000 cm^{-1}) lie outside the obtainable spectral range and are probably present but not observed. The high frequency modes (which are distinguished from adsorbed CO and other contaminants by measuring the frequency shift for deuterium) are attributed to hydrogen atoms bonded to single metal atoms (i.e. bonded at a "top site"). These frequencies are consistent with those for terminally bound hydrogen atoms in metal hydride clusters (1900-2250 cm^{-1}). As discussed

earlier, bridge and hollow sites are thought to be the more favorable hydrogen adsorption sites for hydrogen on low-surface-area metals. Indeed the RAIRS study of H adsorbed on a Pd film shows only lower frequency peaks characteristic of a bridge or hollow site, while the Raman spectroscopy study of H adsorbed on Ni/SiO_2 shows both high (>1200 cm^{-1}) and low (<1200 cm^{-1}) frequency peaks. This confirms that both top site hydrogen atoms and multiply-bonded hydrogen atoms are present on high-surface area, dispersed metals, but the latter sites are not detectable by TAIRS.

IV. Conclusions

Vibrational spectra of hydrogen adsorbed on metal surfaces show that, on both single crystal and high surface area metal surfaces, hydrogen is dissociatively adsorbed. The exact nature of the adsorbed hydrogen atoms is difficult to determine from vibrational spectroscopy alone, but some general trends have been found. The adsorbed state of H atoms is sensitive both to the chemical nature of the metal and to the geometry of the metal. It appears that hydrogen atoms bond preferentially at bridge and hollow sites on "flat" single crystals and thin films, but bonding at top sites also occurs on "rougher" high surface area metals. The observed vibrational frequencies depend more on the structure of the crystal face than on the strength of the metal-hydrogen bond as measured by heats of adsorption. Also, the vibrational frequencies are quite sensitive to changes in bond lengths and bond angles, so that analogous surface sites on different metal surfaces have different vibrational frequencies.

While the vibrational frequencies and bonding geometries of hydrogen atoms on metal surfaces appear in many cases to be analogous to metal hydride clusters, recent vibrational spectra and calculations for H atoms on "smooth"

metal surfaces indicate a unique form of hydrogen adsorbed on surfaces -- "delocalized hydrogen". This delocalized adsorption is more pronounced for hydrogen atoms than other adatoms, because hydrogen's low mass results in a large "zero-point" motion. Since much of the reactivity of surface hydrogen undoubtly occurs from thermally excited atoms, which are particularly delocalized, perhaps one should not think of these atoms as having a well-defined bonding geometry; maybe, just as one thinks of "electron clouds" for electrons, one should think of a "hydrogen cloud" or, more descriptively, of a "hydrogen fog" that covers the surface and is responsible for the reactivity of adsorbed hydrogen atoms.

Experimental techniques for doing vibrational spectroscopy of adsorbates at surfaces are continually being developed and improved. Recent improvements in infrared and Raman spectroscopy should make it possible to extend the vibrational spectroscopy data base for adsorbates on single crystal surfaces in ultra-high vacuum to low and high-surface area metals at high pressures. New directions are now possible, including the study of the reactivity of different types of adsorbed hydrogen by isotopic labelling [58], and determination of the effect of coadsorbed hydrogen on the bonding of other adsorbates [59]. Clever use of vibrational spectroscopy together with a variety of well-chosen catalytic chemical reactions on different surfaces will hopefully enable us to develope an atomic scale understanding of the role of hydrogen in heterogeneous catalysis.

Acknowledgement

We thank Dr. M.A. Van Hove and Prof. L.M. Falicov for helpful discussions in connection with this work. This work was supported by the Director, Office of Energy Research, Office of Basic Energy Sciences, Materials Sciences Division of the U.S. Department of Energy under Contract Number DE-AC03-76SF00098.

References

1. G.T. Haller, Catal. Rev. - Sci. Eng. 23(4) (1981) 477.

2. W.N. Delgass, G.L. Haller, R. Kellerman, and J.H. Lunsford, Spectroscopy in Heterogenous Catalysis, Academic, New York, 1979.

3. M.L. Hair, Infrared Spectroscopy in Surface Chemistry, Dekker, New York, 1967.

4. C.B. Duke, J. Electron Spectrosc. Relat. Phenom. 29 (1983) 1.

5. H. Ibach and D.L. Mills, Electron Energy Loss Spectroscopy and Surface Vibrations, Academic, New York, 1982.

6. P.G. Hall and C.J. Wright, "Neutron Scattering from Adsorbed Molecules, Surfaces, and Intercalates, published in Chemical Physics of Solids and their Surfaces, Vol. 17.

7. R.P. Cooney, G. Lurthoys, and N.T. Tam, Advan. Catalysis 24 (1975) 293.

8. R.K. Chang and T.E. Furtak, eds., Surface Enhanced Raman Scattering, Plenum, New York, 1982.

9. F.M. Hoffmann, Surf. Sci. Reports 3(2/3) (1983) 107.

10. R.P. Eischens and W.A. Pliskin, Adv. Catal. 10 (1958) 1.

11. S. Chiang, R.G. Tobin, and P.L. Richards, Phys. Rev. Lett. 49(23) (1984) 648.

12. R.M. Kroeker and P.K. Hansma, Catal. Rev. - Sci. Eng. 23(4) (1981) 553.

13. F. Trager, H. Coufal, and T.J. Chuang, Phys. Rev. Lett. 49(23) (1982) 1720.

14. A.M. Baro, H. Ibach, and H.D. Bruchmann, Surface Sci. 88 (1979) 384.

15. J.E. Demuth, D. Schmeisser, and Ph. Avouris, Phys. Rev. Lett. 47 (1981) 1166; Ph. Avouris, D. Schmeisser, and J.E. Demuth, Phys. Rev. Lett. 48 (1982) 199; S. Andersson and J. Harris, Phys. Rev. Lett. 48 (1982) 545.

16. H. Froitzheim, Electron Energy Loss Spectroscopy: In Electron Spectroscopy for Surface Analysis, Topics in Current Physics 4, H Ibach Ed., Springer-Verlag, Berlin-Heidelberg-New York (1977), 205-250; H. Ibach, H. Hopster, B. Sexton., Appl. Surface Sci. 1 (1977) 1; B.E. Koel and G.A. Somorjai, Surface Structural Chemistry. Published in Catalysis: Science and Technology Vol. 38 J.R. Anderson, M. Boudart, eds., Springer-Verlag (New York) in press; B.A. Sexton, Appl. Phys. A26 (1981) 1; Ph. Avouris and J.E. Demuth, Ann. Rev. Phys. Chem. 35 (1984) 49.

17. F.M. Propst and T.C. Piper, J. Vac. Sci. Technol. 4 (1967) 53.

18. H. Froitzheim, H. Ibach, and S. Lehwald, Phys. Rev. Lett. 36 (1976) 1549.

19. C. Backx, B. Feuerbacher, B. Fitton, and R.F. Willis, Physics Letters 60A (1977) 145.

20. A. Adnot and J.-D. Carette, Phys. Rev. Lett. 39 (1977) 209.

21. W. Ho, R.F. Willis, and E.W. Plummer, Phys. Rev. Lett. 40 (1978) 1463.

22. M.R. Barnes and R.F. Willis, Phys. Rev. Lett. 41 (1978) 1729.

23. R.F. Willis, Surface Sci. 89 (1979) 457.

24. R.F. Willis, W. Ho, E.W. Plummer, Surface Sci. 80 (1979) 593.

25. W. Ho, N.J. DiNardo, and E.W. Plummer, J. Vac. Sci. Technol. 17 (1980) 134.

26. W. Ho, R.F. Willis, and E.W. Plummer, Phys. Rev. B21 (1980) 4202.

27. B.M. Hall, S.Y. Tong, and D.L. Mills, Phys. Rev. Lett. 50 (1983) 1277.

28. E.F.J. Didham, W. Allison, and R.F. Willis, Surface Sci. 126 (1983) 219.

29. S.R. Bare, P. Hofmann, M. Surman, and D.A. King, Journal of Electron Spectroscopy and Related Phenomena 29 (1983) 265.

30. C.M. Mate and G.A. Somorjai, to be published.

31. G.J. Schulz, Rev. Mod. Phys. 45 (1973) 378.

32. H. Ibach and D.L. Mills, ref. 5, pgs. 116-120.

33. M.W. Howard, U.A. Jayasooriya, S.F.A. Kettle, D.B. Powell and N. Sheppard, Chem. Commun. 929 (1979) 18.

34. Y.J. Chabal, Phys. Rev. Lett., 55(8) (1985) 845; refers to a future publication by J.P. Woods and J.L. Erskine.

35. K. Christmann, R.J. Behm, G. Ertl, M.A. Van Hove, and W.H. Weinberg, J. Chem. Phys. 70 (1979) 4168.

36. M.J. Puska, R.M Nieminen, M. Manninen, B. Chakraborty, S. Holloway, and J.K. Norskov, Phys. Rev. Lett. 51 (1983) 1081.

37. M.J. Puska and R.M. Nieminen, Surf. Sci. 157 (1985) 413.

38. K. Christmann, O. Schover, G. Ertl, and M. Neumann, J. Chem. Phys. 60 (1974) 4528.

39. M.A. Barteau, J.Q. Broughton, and D. Menzel, Surface Sci. 133 (1983) 443; H. Conrad, R. Scala, W. Stenzel, and R. Unwin, J. Chem. Phys. 81 (1984) 6371; P. Feulner and D. Menzel, Surface Sci. 154 (1985) 465.

40. J.T. Yates,Jr., P.A. Thiel, an W.H. Weinberg, Surface Sci. 84 (1979) 427.

41. K. Christmann, G. Ertl, and T. Pignet, Surface Sci. 54 (1976) 365.

42. P.W. Tamm and L.D. Schmidt, J. Chem. Phys. 54 (1971) 4475.

44. S. Andersson, Chem. Phys. Lett. 55 (1978) 185.

44. N.J. DiNardo and E.W. Plummer, Surface Sci. 150 (1985) 89; L. Olle and A.M. Baro, Surf. Sci. 157 (1985) 413; M. Nishijima, S. Masuda, M. Jo, and M. Onchi, J. Electron Spectrosc. Relat. Phenom. 29 (1983) 273.

45. G.B. Blanchet, N.J. DiNardo, and E.W. Plummer, Surface Sci. 118 (1982) 496.

46. C. Backx, B. Feuerbacher, B. Fitton and R.F. Willis, Surface Sci. 63 (1977) 193.

47. A.M. Baro and W. Erley, Surface Sci. 112 (1981) L759; F. Bozso, G. Ertl, M. Grunze, and M. Weiss, Appl. Surface Sci. 1 (1977) 103.

48. F. Zaera, E.B. Kollin, and J.L. Gland, to be published.

49. C. Nyberg and C.G. Tengstal, Phys. Rev. Lett. 50(21) (1983) 1680; C. Nyberg and C.G. Tengstal, Surf. Sci. 126 (1983) 163; K. Christmann and J.E. Demuth, J. Chem. Phys. 76(12) (1982) 6318.

50. A.M. Baro and H. Ibach, Surf. Sci. 92 (1980) 237.

51. P. Nordlander, S. Holloway, and J.K. Norskov, Surf. Sci. 136 (1984) 59.

52. a)H. Jobic and A. Renouprez, J. Chem. Soc., Faraday Trans. 1, 80 (1984) 991; b)A. Renouprez, P. Fouilloux, G. Coudurier, D. Tocchetti, and R. Stockmeyer, Trans. Faraday. Soc. 73 (1977) 1; c)R. Stockmeyer, H.M. Stortnik, I. Natkaniec, and J. Mayer, Ber. Bunsenges. Phys. Chem. 84 (1980) 79; d)R.D. Kelley, J.J. Rush, and T.E. Madey, Chem. Phys. Lett. 66 (1979) 159.

53. J. Howard, T.C. Waddington, and C.J. Wright, J. Chem. Phys. 64 (1976) 3897; J. Howard, T.C. Waddington, and C.J. Wright, Neutron Inelastic Scattering 1977, Vol. II (IAEA Vienna 1978) p.499.

54. J. Howard, T.C. Waddington, and C.J. Wright, Chem. Phys. Lett. 56 (1978) 258.

55. U.A. Jayasooriya, M.A. Chesters, M.W. Howard, S.F.A. Kettle, D.B. Powell, and N. Sheppard, Surface Sci. 93 (1980) 526.

56. W. Krasser and A.J. Renouprez, J. Raman Spectrosc. 8(2) (1979) 92.

57. I. Ratajezykowa, Surf. Sci. 48 (1975) 549.

58. HREEL spectra on single crystal surfaces in UHV after high pressure gas exposures using isotope labelling show promise in following the reactivity of adsorbed hydrogen: B.E. Koel, B.E. Bent, and G.A. Somorjai, Surf. Sci. 146 (1984) 211.

59. Studies have shown that adsorbed H atoms may force changes in the adsorption site of coadsorbed species: P.A. Thiel and W.H. Weinberg, J. Chem. Phys. 73(8) (1980) 4081; G.E. Mitchell, J.L. Gland, and J.M. White, Surface Sci. 131 (1983) 167; ref. 52d.

Table 1. Vibrational spectroscopies used to measure vibrational frequencies of atoms and molecules adsorbed on surfaces

Vibrational Spectroscopy	Principle	Samples	Resolution (cm^{-1})	Spectral Range (cm^{-1})	References
High-Resolution Electron Energy Loss Spectroscopy (HREELS)	Inelastic scattering of low energy (1-150 eV) electrons	single crystals, thin films, and foils in UHV	30-90	100-5000	5
Incoherent Inelastic Neutron Scattering (IINS)	Incoherent inelastic scattering of thermal neutrons	50-100 g of powder	5-50	4-4000	6
Raman Spectroscopy and Surface-Enhanced Raman Spectroscopy (SERS)	Inelastic scattering of photons of visible light	100 mg powder, single crystals, electrodes	1-10	200-5000	7,8,1
Reflection Absorption Infrared Spectroscopy (RAIRS)	Absorption of infrared radiation detected in the reflected beam	foils, single crystals	1-10	700-5000	9
Transmission Absorption Infrared Spectroscopy (TAIRS)	Absorption of infrared radiation detected in the transmitted beam	10-100 mg pressed powder, solution	1-10	400-5000	10,1-3
Infrared Emission Spectroscopy (IES)	Detection of the emitted black body radiation from vibrating molecules	foils, single crystals, zeolite on a Au wire	1-10	400-4000	11,1
Inelastic Electron Tunneling Spectroscopy (IETS)	Inelastic tunneling of electrons between metals through an oxide layer containing the sample	1-10 mg Al or other metal oxide (20 Å thick supported on metal film)	10-50	10-5000	12
Photoacoustic Spectroscopy (PAS)	Vibrational excitation with pulsed light source and detection of the sound waves generated	100 mg powder or metal film	1-10	400-5000	13

Table 2

Calculated bandcenters (bandwidths) in cm^{-1} for hydrogen on Ni(111). From Puska et al [36,37].

A_1^0	A_1^1	A_1^2	E^1	E^2
16 (32)	597 (347)	1113 (323)	323 (210)	1095 (768)

Experimentally measured transition energies by HREELS (cm^{-1}) and heats of adsorption (kcal/mole) for hydrogen adsorbed on hexagonally close-packed surfaces.

Surface	ref.	$A_1^0 \rightarrow A_1^1$	$A_1^0 \rightarrow A_1^2$	$A_1^0 \rightarrow A_1^3$	$A_1^0 \rightarrow E^1$	$A_1^0 \rightarrow E^2$	Heats of adsorption
Ni(111)	[25,38]	710	1120	--	--	--	23
Ru(001)	[39]	690 (low θ)	1070	--	--	--	29
		820 (high θ)	1140	1550			
Rh(111)	[30,40]	750	1100	1430	400	1280	19
Pt(111)	[14,41]	550	1230	--	--	--	9.5

Table 3. Frequencies observed by HREELS for adsorbed hydrogen.

Metal surface	ref.	frequencies (cm^{-1})	Proposed Adsorption site	Heat of Adsorption (kcal/mole)
W(100)	[23,42]	440, 960, 1215 (low coverage, reconstructed)	bridge	32
		680, 1000, 1280 (high coverage, unreconstructed)	bridge	
W(110)	[42,45]	645, 775, 1290	long bridge	33
W(111)	[42.46]	1290	top	37
Fe(110)	[47,48]	880, 1060	short bridge	26
Mo(100)	[48]	1125, 1240-1260 (low coverage, reconstructed)	several bridge sites	24
		555, 1030, 1125 (high coverage, unrecontructed)	bridge	
Ni(100)	[38,43]	595	four-fold hollow	23
Ni(110)	[38,44]	650, 1060 (low coverage, unreconstructed)	bridge and three-fold hollow	22
		610, 940 (high coverage, reconstructed)	several bridge sites	
Pd(100)	[49]	515	four-fold hollow	21
Pt[6(111)x(111)]	[50]	500, 1130, 1270	three-fold hollow, and bridge	12

Table 4. Frequencies (cm^{-1}) observed by IINS for adsorbed hydrogen.

Raney Nickel [52]		platinum black [53]	palladium black [54]
low coverage	high coverage		
		2000-2250	
		1696	
1080	1100	1296	
	940	936	916
780		856	823
	600-640	616	
	400	512	

Table 5. Frequencies observed by TAIRS, RAIRS, and Raman spectroscopy for hydrogen adsorbed on dispersed metal surfaces.

Metal/support	Spectroscopy	Reference	ν_{M-H} (cm^{-1})	ν_{M-D} (cm^{-1})
Pt/Al_2O_3	TAIRS	[55]	2120, ~2060	1520, 1490
Ir/Al_2O_3	TAIRS	[55]	2120, ~2050	1520, 1490
Ni/Al_2O_3	TAIRS	[55]	1880	1360
Fe, Co, Ni, Rh, Pd and Ir/Al_2O_3	TAIRS	[55]	1850-1940	--
Ni/SiO_2	Raman	[56]	2028, 1999 1600, 950 725, 692	1410, 1380 1150, 740 -- , --
Pd film	RAIR	[57]	760, 880	-- , --

Figure Captions

Figure 1: Top views of the atomic arrangement in the first two or three layers of the common low-Miller-index faces of face-centered cubic (fcc), body-centered cubic (bcc), and hexagonal close-packed (hcp) crystals. Thin-lined atoms are behind the plane of thick-lined atoms. For the "open" bcc(111) crystal face, second layer atoms are dotted and third layer atoms are slashed. High symmetry binding sites are indicated.

Figure 2: Schematic diagram of a typical high-resolution electron energy loss spectrometer. The energy dispersive elements are 127° cylindrical sectors.

Figure 3: Normalized electron energy loss spectra for a saturation coverage of H chemisorbed on W(100) for $\theta_i = 23^\circ$ incident angle and an impact energy $E_o = 9.65$ eV showing the different vibrational losses observable in (a)the specular beam direction and (b) the +17° off-specular direction. [From Ho et al (ref. 21), used with permission.]

Figure 4: Absolute intensities of the energy loss peaks in Figure 3 as a function of collection angle away from the specular direction $\Delta\theta_s$. The scattering geometry is shown in the upper inset. [From Ho et al (ref. 21), used with permission.]

Figure 5: High-resolution electron energy loss vibrational spectra taken, in the specular direction, at three different incident electron beam energies for H_2 dissociatively adsorbed on Rh(111) at 77 K. The intensity variations are the result of "resonant" impact scattering of the electrons at an incident beam energy of ~4.7 eV.

Figure 6: Absolute intensities in the specular direction of the elastic peak and of the energy loss peaks in Figure 5 as a function of incident electron beam energy for H on Rh(111) at 77 K. Note that both the elastic peak and the energy loss peak for .001 monolayer of coadsorbed CO are at low intensity for E = 4.7 eV where the H energy loss peaks are strongly enhanced by "resonant" impact scattering.

Figure 7: Plot of the M-H bond stretching frequency ratio (ν_{as}/ν_s) observed in the infrared spectra of bridged metal hydrides versus the tangent of half the interbond M-H-M angle, α. The ν_{as}/ν_s ratio determined by HREELS for chemisorbed, bridge-bonded H on the unreconstructed [p(1x1)H] and reconstructed [c(2x2)H] W(100) surfaces is plotted on the theoretical fit [$\tan(\alpha/2) = \nu_{as}/\nu_s$ ($k_{MH} \cong 108$ N/m)] to determine the surface bonding geometry shown in Figure 8. [From R.F. Willis (ref. 23), used with permission.]

Figure 8: Side view of the bridge-bonding geometry of H on (a)unreconstructed [p(1x1)H] W(100) and (b)reconstructed [c(2x2)H] W(100) as determined by comparison to metal hydride clusters as shown in Figure 7 [23].

Figure 9: Potential, A_1 wave functions, and densities for hydrogen chemisorbed on the Ni(100) surface. The left panel shows the potential and wave functions in a vertical plane along the <110> direction through the fourfold center position where the potential has its minimum. The lengths of the cuts are the Ni nearest-neighbor distance ($4.7a_o$) both in the parallel and the perpendicular directions. At the top of the right panel, the potential is shown in a cut parallel to the surface through the absolute minimum. Underneath are shown the hydrogen densities, integrated perpendicular to the surface in the same parallel cut. In the right panel the cuts are one Ni lattice constant ($6.65\ a_o$) in each direction. All wave functions are evalutated at Γ. [From Puska et al (ref. 36), used with permission.]

Figure 10: The band structure for hydrogen chemisorbed on the Ni(100) surface shown along the high-symmetry directions indicated in the inset. Only the states belonging to the A_1 representation of the C_{4v} point group are shown. The zero of energy is the ground-state energy (-2.6 eV) at the Γ point. This includes a zero-point energy of 0.1 eV. In the inset the Brillouin zone has been rotated 45^o relative to the convention used in Figure 9. [From Puska et al (ref. 36), used with permission.]

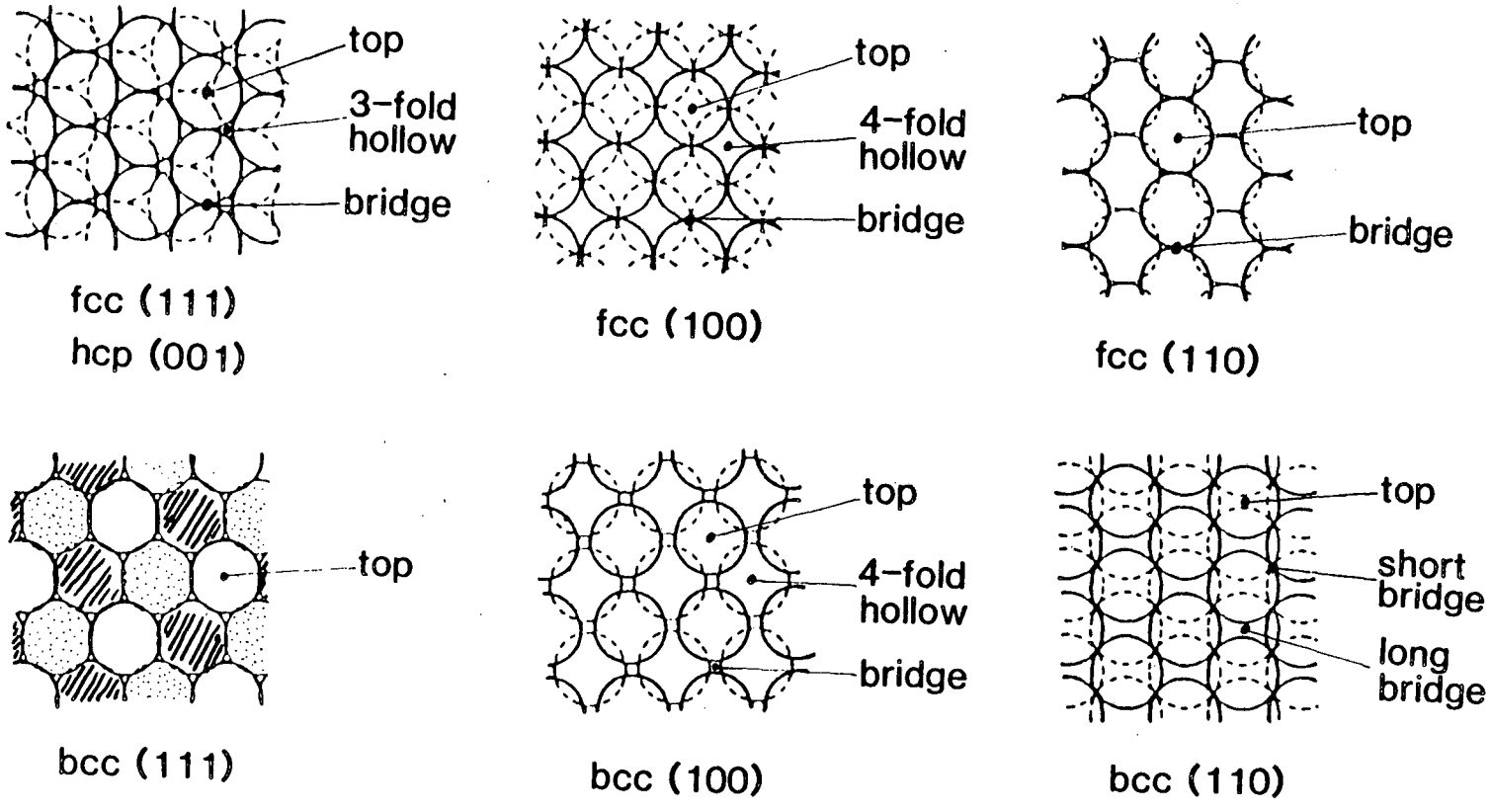

XBL 859-4054

Fig. 1

HIGH-RESOLUTION ELECTRON ENERGY LOSS SPECTROMETER

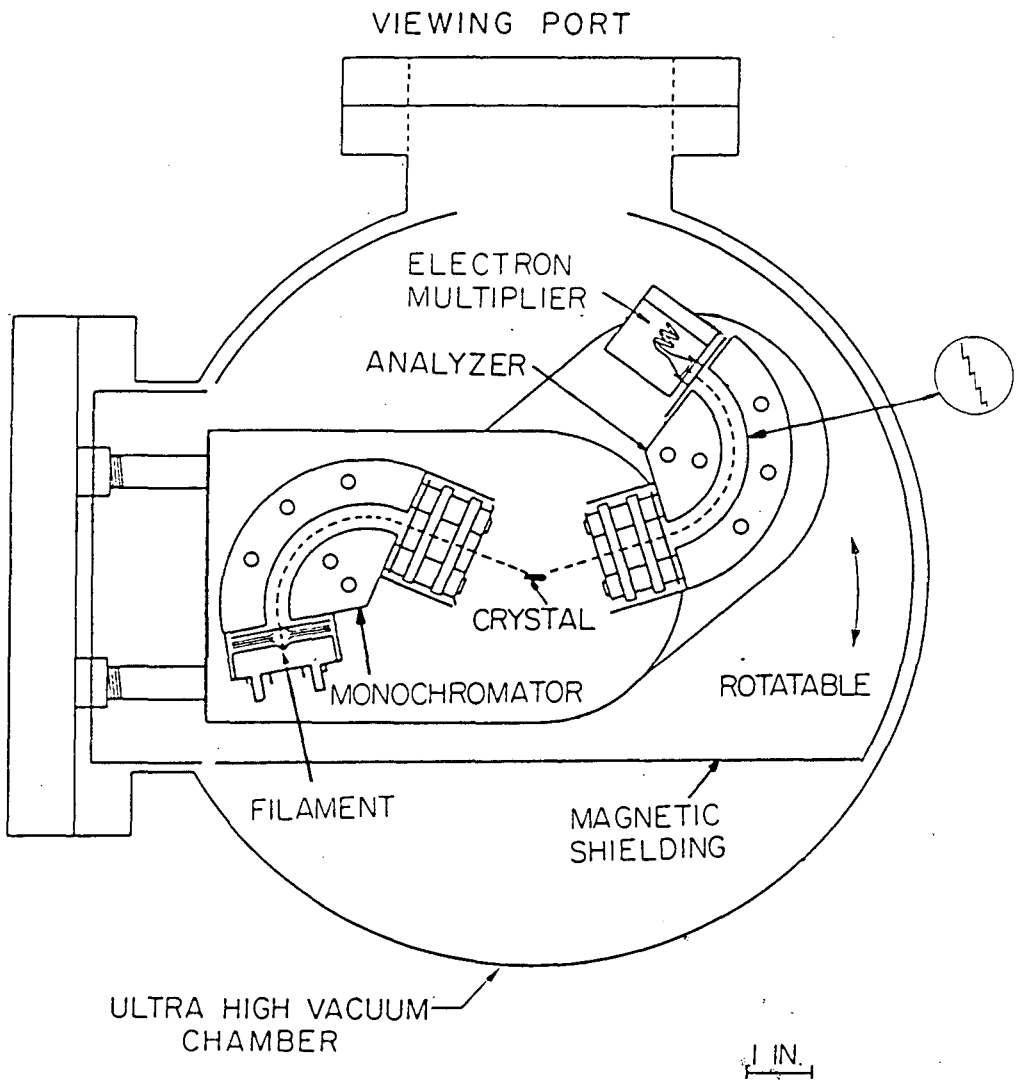

XBL 857-2942

Fig. 2

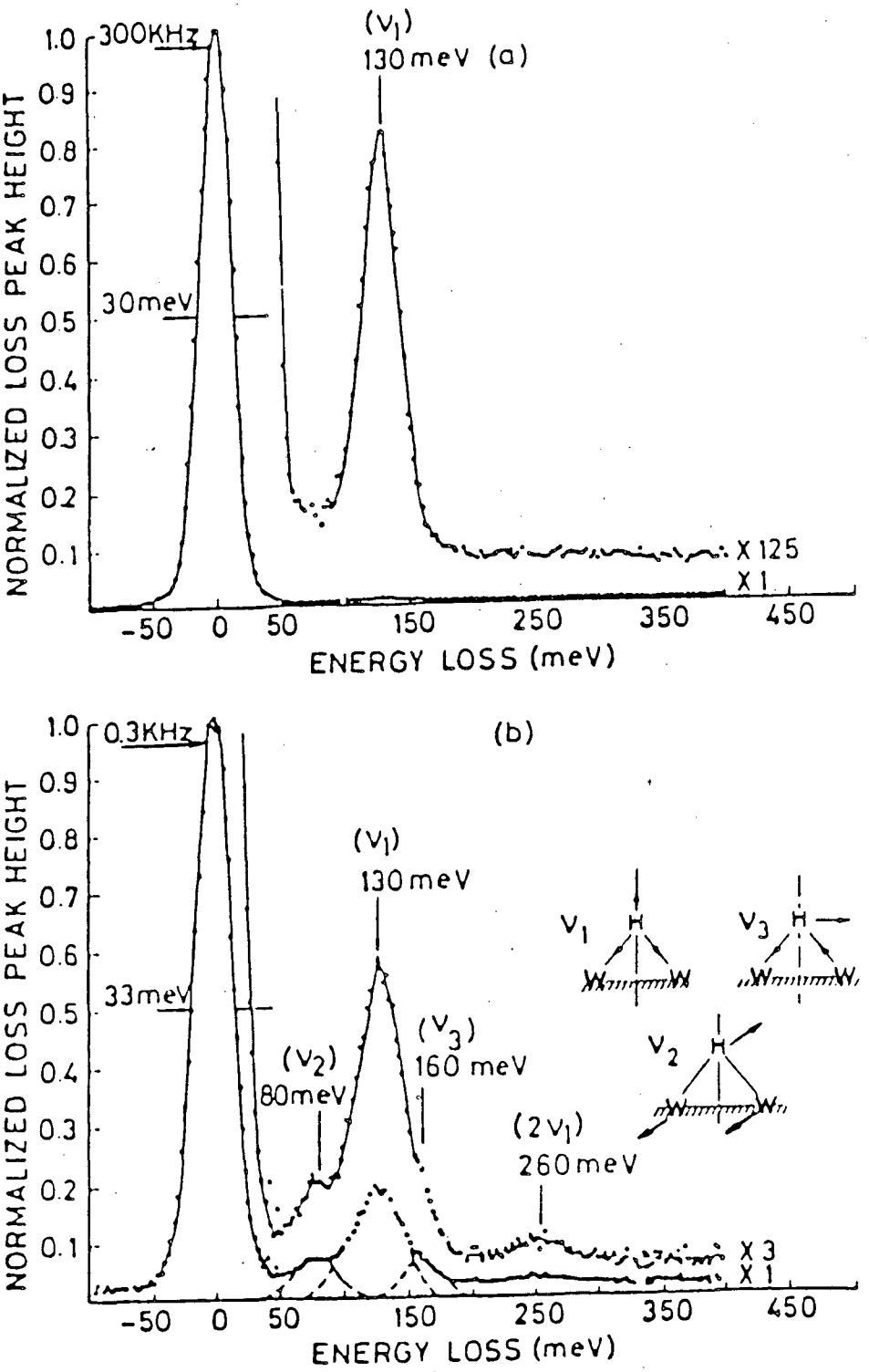

XBL 859-4037

Fig. 3

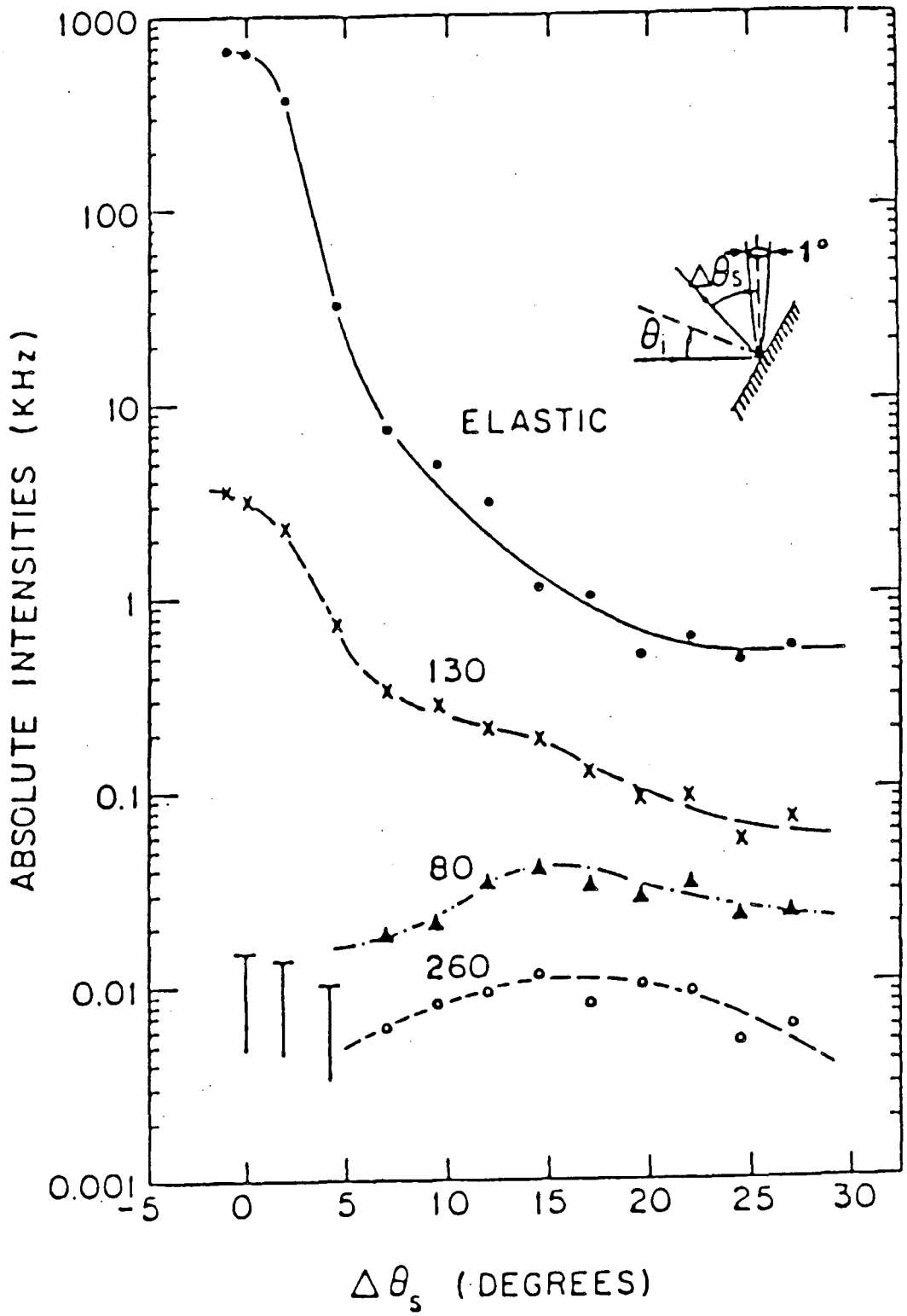
1000
100
10
1
0.1
0.01
0.001
ABSOLUTE INTENSITIES (KHz)
ELASTIC
130
80
260
1°
$\Delta\theta_s$
θ_i
-5
0
5
10
15
20
25
30
$\Delta\theta_s$ (DEGREES)
XBL 859-4038

Fig. 4

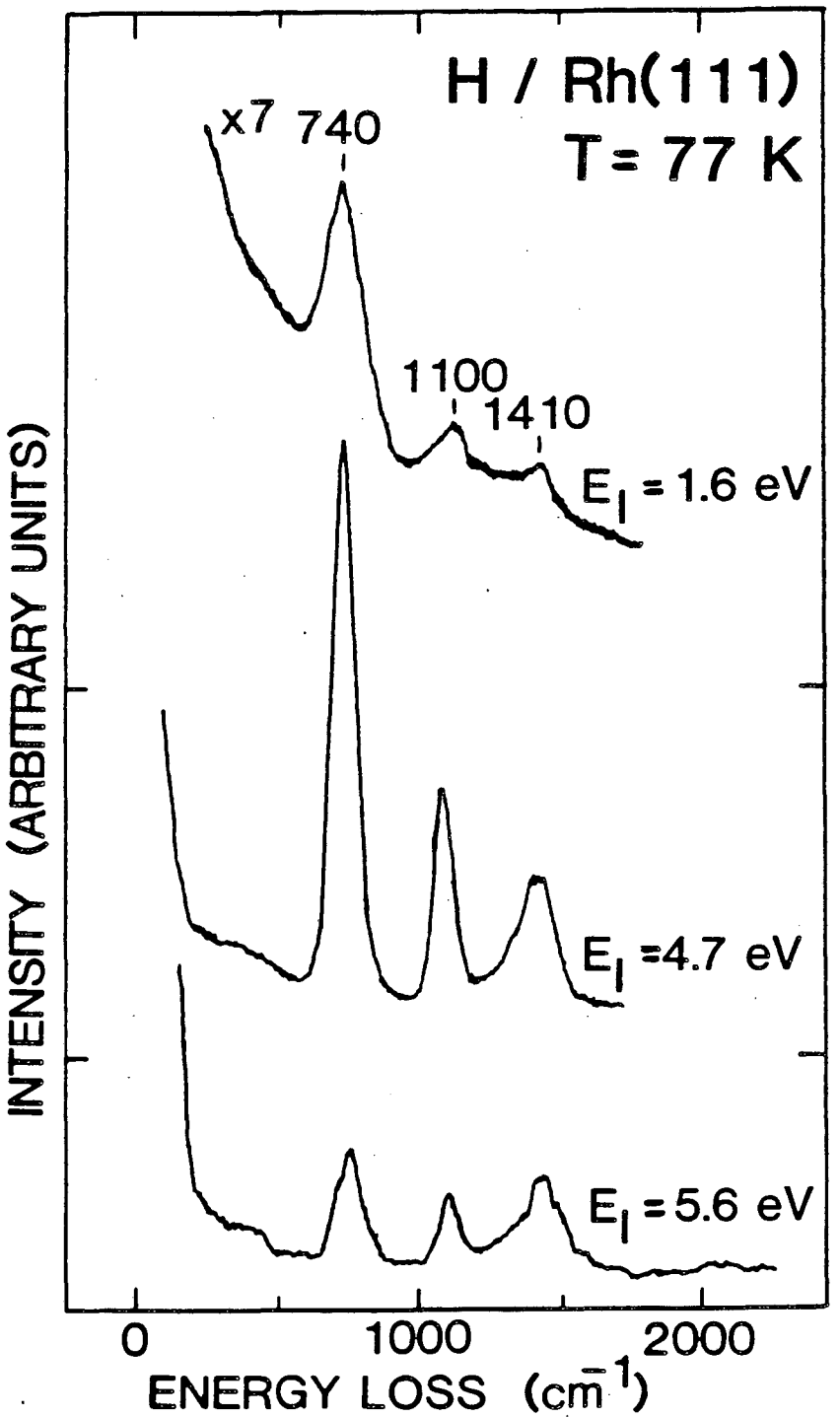

XBL 859-4039

Fig. 5

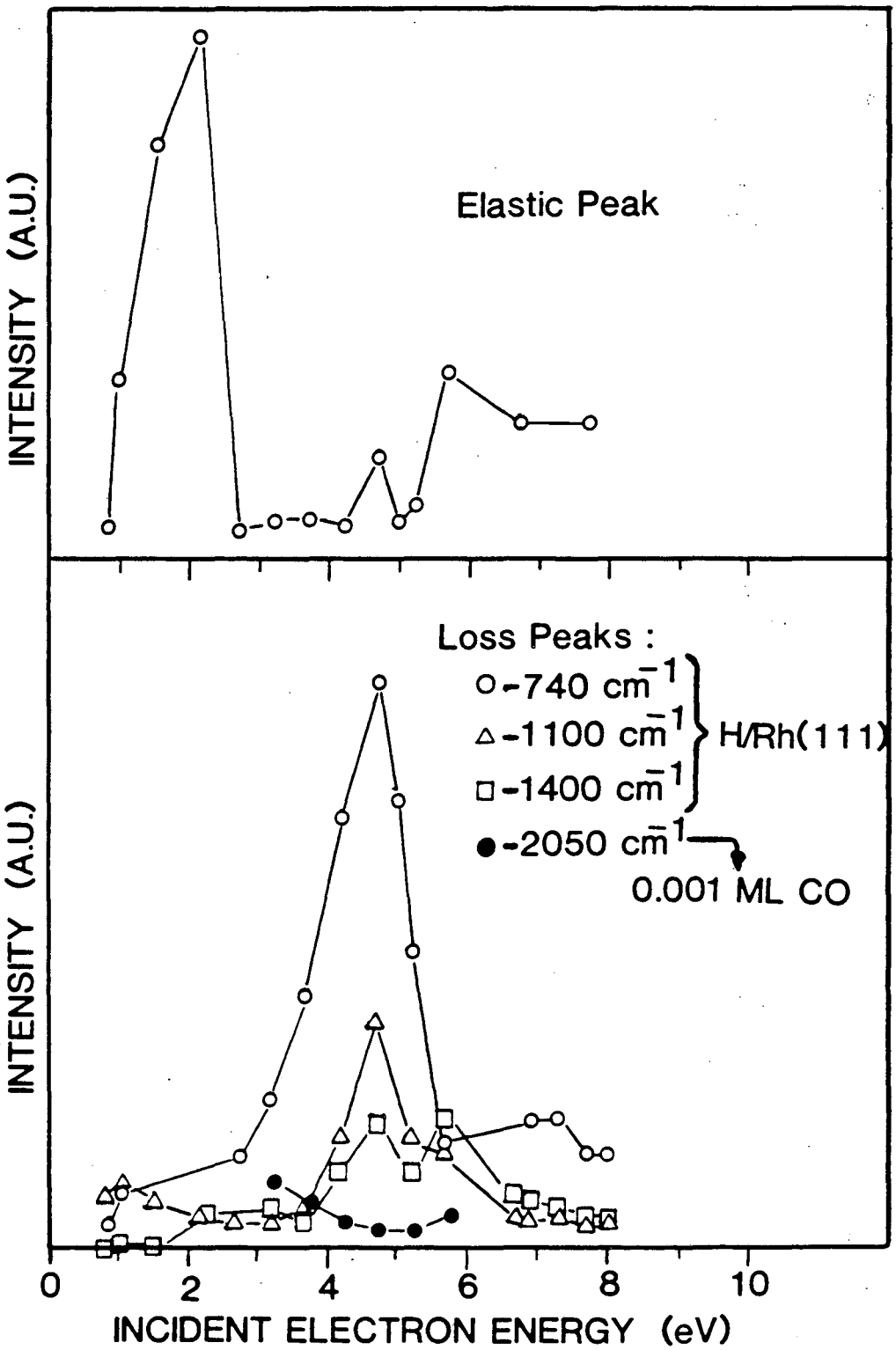

XBL 859-4040

Fig. 6

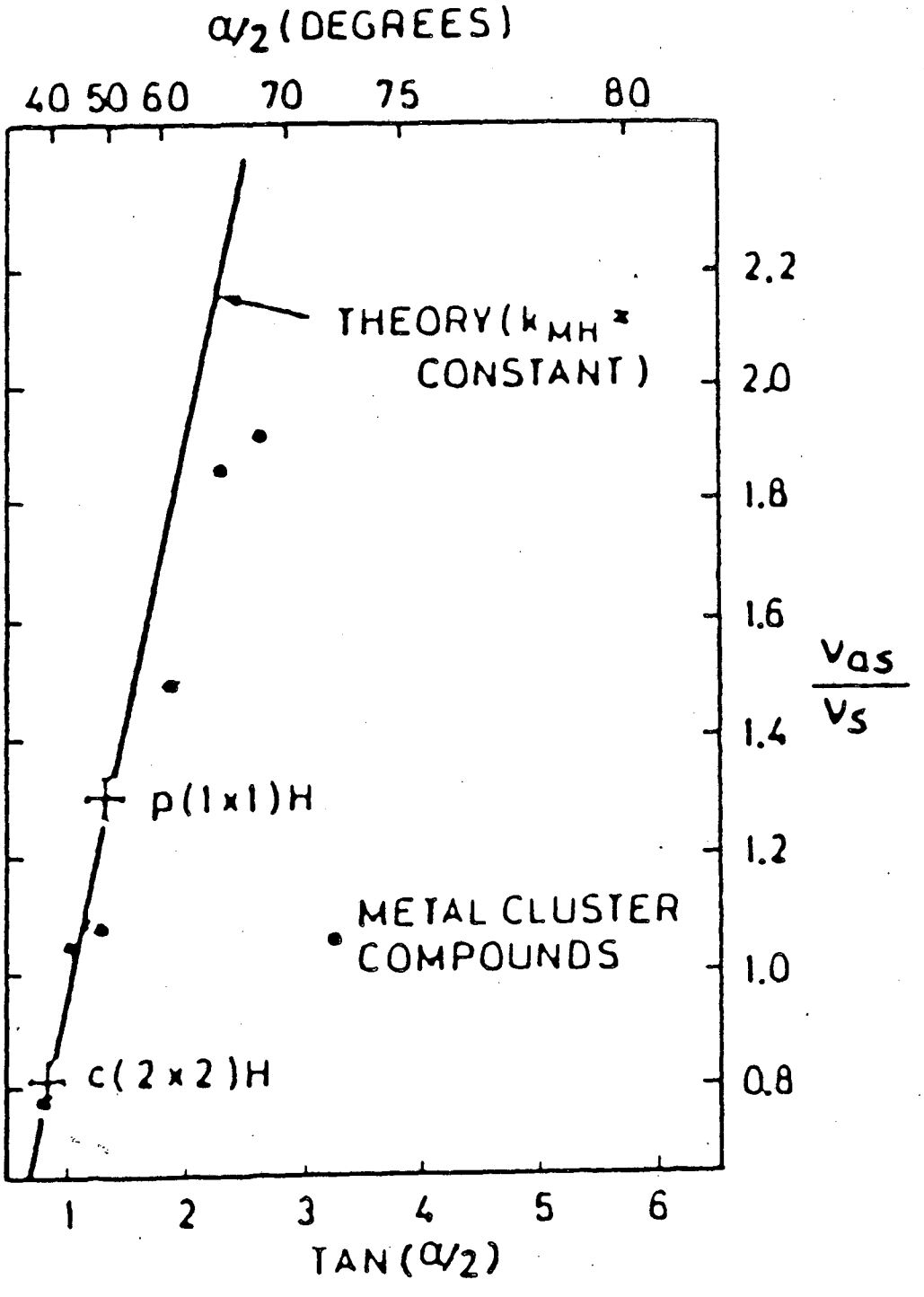

XBL 859-4041

Fig. 7

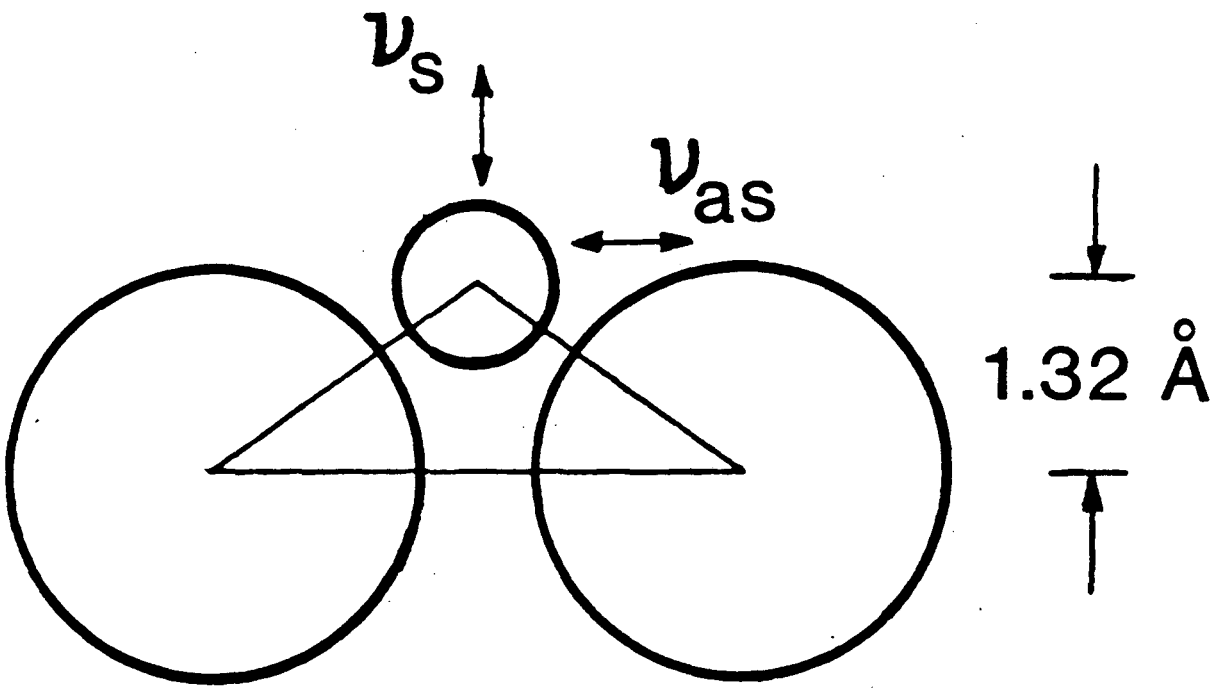

W(100) p(1x1)H

d_{WH}= 2.05±0.05 Å

(A)

XBL 859-4044

Fig. 8A

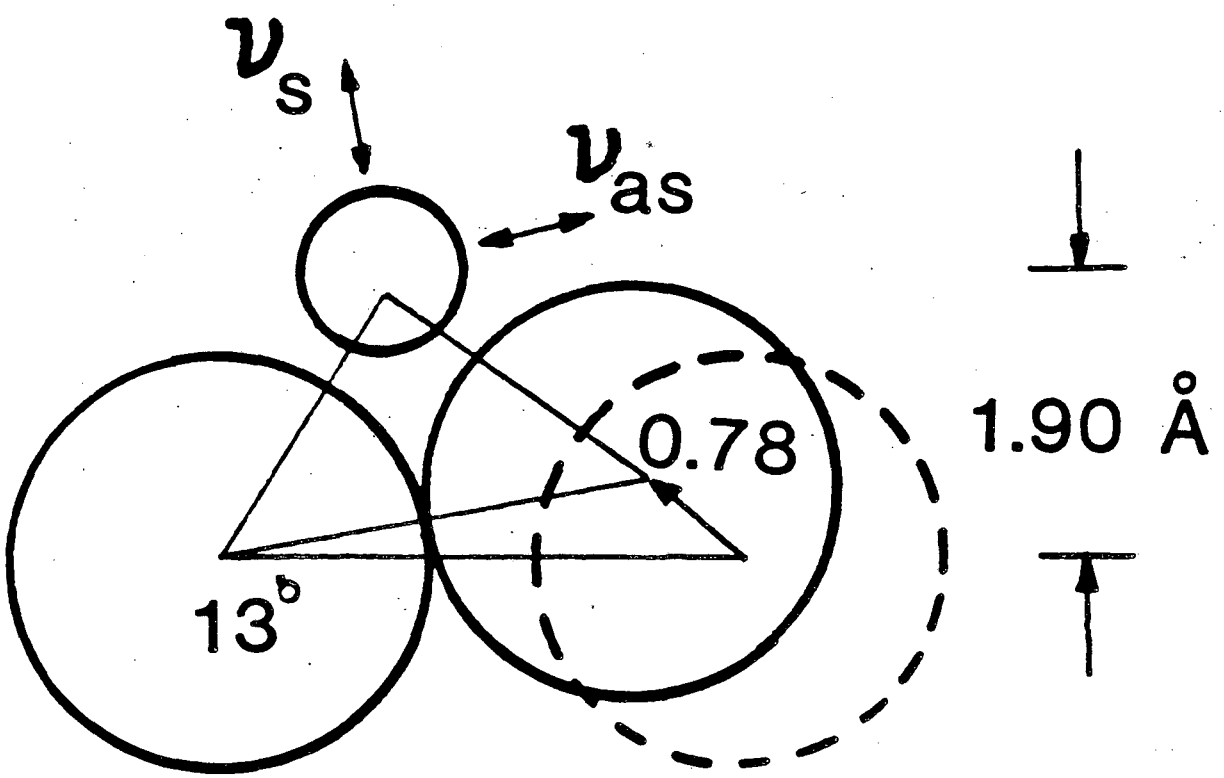

W(100)c(2x2)H

d_{WH}= 2.15± 0.05 Å

(B)

XBL 859-4045

Fig. 8B

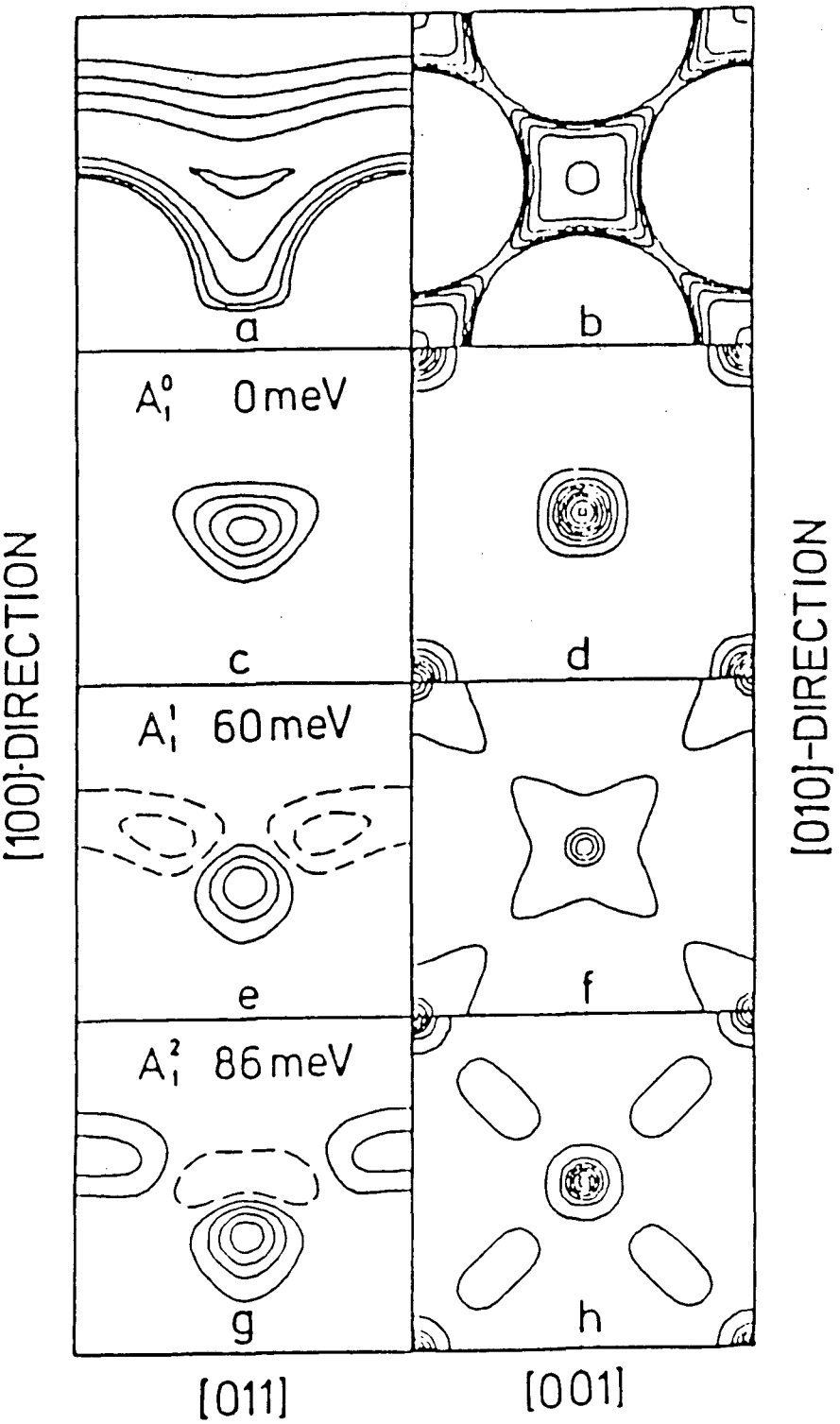

XBL 859-4042

Fig. 9

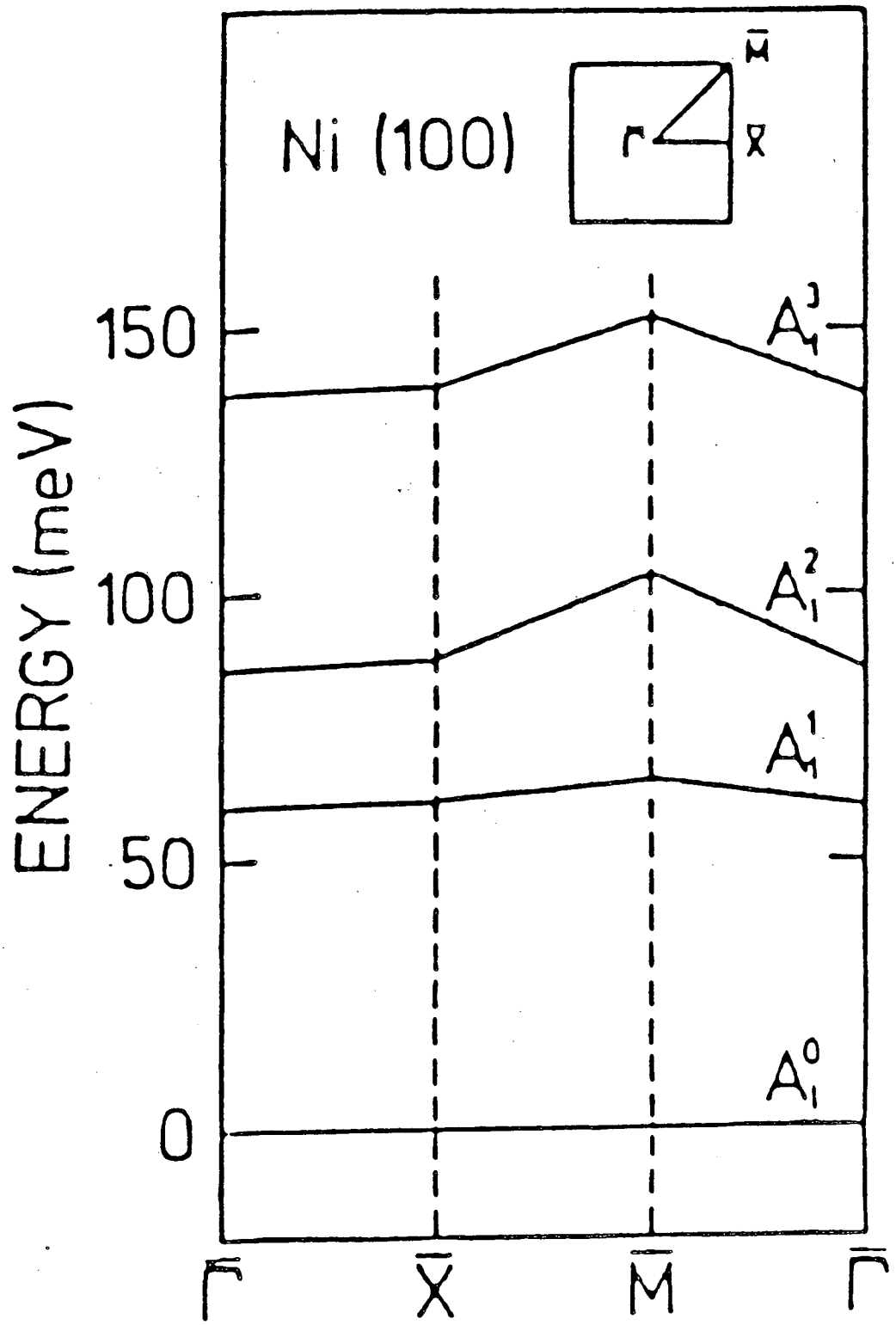

XBL 859-4046

Fig. 10

This report was done with support from the Department of Energy. Any conclusions or opinions expressed in this report represent solely those of the author(s) and not necessarily those of The Regents of the University of California, the Lawrence Berkeley Laboratory or the Department of Energy.

Reference to a company or product name does not imply approval or recommendation of the product by the University of California or the U.S. Department of Energy to the exclusion of others that may be suitable.

LAWRENCE BERKELEY LABORATORY
TECHNICAL INFORMATION DEPARTMENT
UNIVERSITY OF CALIFORNIA
BERKELEY, CALIFORNIA 94720